

involve

a journal of mathematics

Mathematical modeling of
a surface morphological instability of
a thin monocrystal film in a strong electric field

Aaron Wingo, Selahittin Cinar, Kurt Woods and Mikhail Khenner



Mathematical modeling of a surface morphological instability of a thin monocrystal film in a strong electric field

Aaron Wingo, Selahittin Cinar, Kurt Woods and Mikhail Khenner

(Communicated by Natalia Hritonenko)

A partial differential equation (PDE)-based model combining the effects of surface electromigration and substrate wetting is developed for the analysis of the morphological instability of a monocrystalline metal film in a high temperature environment typical to operational conditions of microelectronic interconnects and nanoscale devices. The model accounts for the anisotropies of the atomic mobility and surface energy. The goal is to describe and understand the time-evolution of the shape of the film surface. The formulation of a nonlinear parabolic PDE problem for the height function $h(x, t)$ of the film in the electric field is presented, followed by the results of the linear stability analysis of a planar surface. Computations of a fully nonlinear evolution equation are presented and discussed.

1. Introduction

The drift of ionized adsorbed atoms (adatoms) on a metal or semiconductor crystal surface due to their interaction with the “electron wind” is termed *surface electromigration*. The “wind” force on adatoms is the effect of a high-density direct current through the bulk of a crystal, which also heats up the surface—thus increasing the adatoms’ own kinetic energy. It is this combination that makes adatoms drift. Surface electromigration was studied theoretically in connection to the grain-boundary grooving in polycrystalline films [Averbuch et al. 2001; Maroudas 1995], the kinetic instabilities of crystal steps [Chang et al. 2006; Debierre et al. 2007; Stoyanov 1997], morphological stability of thin films [Dobbs and Krug 1994; Krug and Schimschak 1997; Barakat et al. 2012; Khenner 2013], and recently, as a way to fabricate nanometer-sized gaps in metallic films—suitable for testing of the conductive properties of single molecules and control of their functionalities [Barnes et al. 2010; Bolotin et al. 2007; Block et al. 2006]. Although the phenomenon of electromigration has been known for over 100 years, it became of practical interest

MSC2010: 35R37, 35Q74, 37N15, 65Z05, 74H55.

Keywords: nonlinear evolution PDEs, electromigration, surface diffusion, morphology, stability.

in 1966 when the first integrated circuits became commercially available. It is considered a key factor in determining the reliability of integrated circuits.

As we just mentioned, one recent technological application of electromigration is the fabrication of the nanoscale contacts (gaps) that are manufactured from the thin Ag films wetting the Si substrate [Barnes et al. 2010; Bolotin et al. 2007; Block et al. 2006]. The gap between contacts can be cyclically opened and closed. To open the contact, a strong electric current is applied at a low temperature of the film (~ 80 K), which enables the surface mass flow of adatoms across the narrow bridge, thus connecting the anode and the cathode, until the bridge breaks. To close the contact, the natural surface diffusion of adatoms across the gap is enabled by heating the film to the room temperature, all the while keeping the electric current.

Another example, more relevant to the present study, is a faceting of the initially planar surface of a crystalline thin film upon passing the current along the substrate. This way the so-called quantum wires can be fabricated [Dai et al. 2014]. Since the cross-section of a quantum wire is only a few nanometers, it possesses very special electronic properties, which makes it desirable for integration into nanoscale devices.

Here we further develop the PDE-based mathematical model of the film-surface morphological instability and evolution driven by the electromigration [Khenner 2013]. The very special feature of the presented model is that it accounts both for the wetting and the surface energy anisotropy effects. The surface morphological instability and evolution in a thin film system where the wetting, anisotropy, and electromigration are active have not been addressed theoretically, although PDE-based models of wetting and anisotropy [Davis et al. 2004; Gill and Wang 2008; Khenner 2008a; 2008b; Khenner et al. 2011], wetting and electromigration [Khenner 2013], and electromigration and anisotropy [Barakat et al. 2012] have been published.

The wetting effect emerges due to the existence of the attractive force between the adatoms and the substrate atoms; this force is nonnegligible because of the very small thickness of the film ($h \sim 10$ nm). The surface-energy anisotropy effect emerges due to the crystal nature of the film surface. The combination of the two effects results in a complicated nonlinear evolution PDE. We use the approach of [Khenner 2013] to build and analyze the model with the added anisotropy effect; first, the governing PDE is derived, and then we analytically obtain the stability regions of the planar surface in the space of the physical parameters and, for the values of the parameters such that the planar surface is unstable, compute the evolution of the small, one-wavelength surface perturbation on a periodic domain. The typical evolution scenarios, such as the evolution to a steady-state or the lateral surface drift, are presented.

2. Problem statement

We assume a simple one-dimensional geometry, where the surface is an open curve (without overhangs) in the xz -plane, described by a function $z = h(x)$. Since the

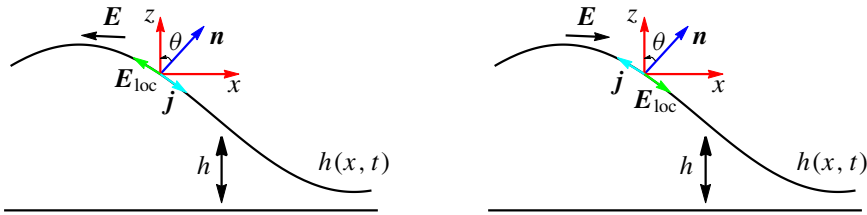


Figure 1. Sketch of the film surface $h(x, t)$ in the horizontal, constant electric field E . Here $E_{\text{loc}} = E \cos \theta$ is the projection of E on the surface. The surface atomic flux j is in the direction opposite to E_{loc} .

curve deforms with time, h is also a function of time t ; that is, $z = h(x, t)$. As is common in physics literature, the curve $h(x, t)$ is termed the *film surface* in the following, despite being a one-dimensional object.

Following [Khenner 2013], we focus on the case of the horizontal electric field (directed along the substrate and the initially planar film surface $h(x, 0) = \text{const.}$). As was stated in the Introduction, we will incorporate the effects of substrate wetting by the film [Khenner 2008a], the anisotropy of the diffusional mobility $M(\theta)$ [Krug and Schimschak 1997], and weak anisotropy of the surface energy $\gamma(\theta)$ [Liu and Metiu 1993], where θ is the angle that the unit normal \mathbf{n} to the surface makes with the vertical coordinate axis z . From the mathematical standpoint, these effects will manifest in our model through various linear and nonlinear terms in the parabolic PDE for $h(x, t)$. The physicomathematical framework in which our model is firmly rooted has been established, beginning in 1960s, through the efforts of many prominent materials scientists, physicists, and mathematicians [Mullins 1963; Cahn et al. 1992; Cahn and Taylor 1994; Di Carlo et al. 1992; Dobbs and Krug 1994; Liu and Metiu 1993; Davis et al. 2004]. The mathematics of the accounting for the relevant physical effects are summarized below, and the physical foundations, as well as further mathematical detail, can be found in the cited papers. To illustrate the effects of the electromigration on film morphology, Figure 1 depicts two directions of the electric field. In Figure 1 (left), the electric current forces the adatoms downhill (from the crest to the trough); thus the surface becomes more planar with time. In Figure 1 (right), the field in the opposite direction forces the adatoms uphill (from the trough to the crest) and thus the surface becomes less planar. This is the instability mechanism that we are investigating in this paper.

The dimensionless PDE governing the evolution of $h(x, t)$ has the form

$$h_t = B[M(h_x)(1 + h_x^2)^{-1/2}\mu_x]_x + A[M(h_x)(1 + h_x^2)^{-1/2}]_x. \quad (1)$$

In (1), $B > 0$ is the effective diffusivity of adatoms and $A \geq 0$ is the strength of the electric field. The first term on the right-hand side stems from the natural diffusion of adatoms (in the absence of the electric current) on a heated crystal surface. The

meaning of this term is that relocation of adatoms through diffusion changes the shape of the surface. It was first derived by Mullins [1963] in what is now considered the classical work. Similarly, the second term stems from the forced diffusion (drift) of adatoms caused by the electromigration force. It was derived in several papers, including [Dobbs and Krug 1994; Krug and Schimschak 1997; Khenner 2013]. The surface chemical potential $\mu(x, t)$ entering the Mullins term contains, in our model, the contributions from wetting (through the dependence of the surface energy γ on the film thickness h ; see (3) below) and anisotropy. The expression for $\mu(x, t)$ reads

$$\mu = (\gamma + \gamma_{\theta\theta})\kappa + (\gamma_h - h_x \gamma_{h\theta}) \cos \theta, \quad \cos \theta = (1 + h_x^2)^{-1/2}, \quad \kappa = -h_{xx} (1 + h_x^2)^{-3/2}. \quad (2)$$

Here κ is the curvature, and $\gamma(h, \theta)$ is the weakly anisotropic film-surface energy (tension):

$$\gamma(h, \theta) = 1 + \epsilon_\gamma \cos 4\theta + (G - 1 - \epsilon_\gamma \cos 4\theta)e^{-h}, \quad \theta = \arctan h_x, \quad (3)$$

where $G > 1$ and $0 \leq \epsilon_\gamma < \frac{1}{15}$ are the parameters; G is the ratio of the (dimensional) substrate energy to the (dimensional) surface energy, and ϵ_γ is the strength of the anisotropy. The interval for ϵ_γ implies that the “stiffness” $\gamma + \gamma_{\theta\theta}$ is larger than 0 for all θ in (2) when $\gamma = \gamma(\theta) = 1 + \epsilon_\gamma \cos 4\theta$ (the four-fold anisotropy typical for most semiconductor and metal crystals). This implies a negative effective “diffusivity” α_1 in the linearized PDE (1) (for $A = 0$): $h_t = \alpha_1 h_{xxxx}$, where $\alpha_1 < 0$. Such a linear PDE is well-posed; i.e., it is forward parabolic. If $\epsilon_\gamma \geq \frac{1}{15}$ (strong anisotropy, typical at comparatively low temperatures), then the PDE is backward parabolic for some θ -intervals and the regularization is required; usually the curvature-squared term is added to $\gamma(\theta)$ [Di Carlo et al. 1992], which raises the PDE order from the fourth to the sixth. In the presence of the electric current, the crystal temperature is high due to Joule heating, which justifies the restriction of the consideration to mild anisotropy. The choice $G > 1$ means that only wetting films are considered; i.e., the substrate energy is larger than the surface energy. Thus dewetting, meaning the substrate exposure, may occur only through the application of the external force, such as the electromigration.

The form of (3) results from the consideration of the conventional “two-layer” model for the film energy; for the discussion of that model see, for instance, [Davis et al. 2004] and the references therein. The parameters and their typical range of values are displayed in Table 1. Notice that the classical Mullins model assumes $\gamma = \text{const.}$ (the isotropic case without the wetting effect); thus the chemical potential reduces to $\mu = \gamma\kappa$. The form of the wetting potential contribution to the surface energy, $(\gamma_h - h_x \gamma_{h\theta}) \cos \theta$, is well established and is taken from [Davis et al. 2004].

In reference to the electromigration term in (1),

$$M(h_x) = \frac{1 + \beta \cos^2(N(\arctan h_x + \phi))}{1 + \beta \cos^2(N\phi)}, \quad \text{where } \beta, N, \phi = \text{const.}, \quad (4)$$

Physical parameters	Typical values	Range	Physical meaning
B	8	fixed	effective adatoms diffusivity
$M(0)$	1	fixed	adatoms mobility on the horiz. surface
h_0	3	$0 \leq h_0 \leq 20$	initial height of the film (same for all x)
A	72	$10 \leq A \leq 1000$	strength of the electric field
G	2	$1 < G \leq 100$	ratio of the substrate energy to the surface energy
$M'(0)$	-3	$-10 \leq M'(0) \leq 0$	derivative of adatoms' mobility on the horiz. surface

Table 1. Values of the dimensionless physical parameters. The definitions of these parameters in terms of the dimensional quantities can be found in [Khenner 2013; 2008b; Khenner et al. 2011]. The typical values in the second column result from the substitutions in these expressions of the published standard values of the dimensional parameters [Mullins 1963; Maroudas 1995; Dobbs and Krug 1994; Krug and Schimschak 1997; Davis et al. 2004; Liu and Metiu 1993], which have been measured in the experiments.

is the anisotropic diffusional mobility (notice that the denominator of the fraction is a constant value for the given nonnegative parameters β , N and ϕ); here β is the anisotropy strength, N is the number of crystallographic symmetry axes and ϕ is the angle between a symmetry direction and the average surface orientation. In this paper, β varies (resulting in a variation of $M'(0)$; see Table 1), $N = 4$, and $\phi = \pi/16$. Notice that $M(0) = 1$ for any β , N , ϕ . Equation (4) is taken from [Krug and Schimschak 1997].

Next, we begin by linearizing $M(h_x)$ about $h_x = 0$; i.e., we write $M(h_x) = M(0) + M'(0)h_x$, where $M(0)$ and $M'(0)$ will be later calculated from (4) for given β , N and ϕ (see [Khenner 2013]). Then

$$\frac{\partial M(h_x)}{\partial x} = \frac{\partial M(h_x)}{\partial h_x} h_{xx} = M'(0)h_{xx}, \tag{5}$$

and (1) now reads

$$h_t = BM'(0)h_{xx}(1 + h_x^2)^{-1/2}\mu_x + B(M(0) + M'(0)h_x)[(1 + h_x^2)^{-1/2}\mu_x]_x + AM'(0)h_{xx}(1 + h_x^2)^{-1/2} + A(M(0) + M'(0)h_x)[(1 + h_x^2)^{-1/2}]_x. \tag{6}$$

In order to compute μ_x in (6), we first calculate $\gamma_{\theta\theta}$, γ_h , $\gamma_{h\theta}$ using (3). Then we substitute these expressions in (2), use the trigonometric identities

$$\cos 4\theta = 8(\cos^4\theta - \cos^2\theta) + 1, \quad \sin 4\theta = 4 \sin \theta \cos \theta (2 \cos^2\theta - 1),$$

(where $\cos \theta = (1 + h_x^2)^{-1/2}$ and $\sin \theta = h_x(1 + h_x^2)^{-1/2}$) and obtain $\mu(x, t)$ in terms of h_x , h_x^2 , h_{xx} , etc. We then substitute $\mu(x, t)$ into (6) and the remaining differentiations are performed.

Finally, we employ the small-slope approximation. The spatial derivatives are replaced as $\partial/\partial x^k \rightarrow \epsilon^k \partial/\partial x^k$, the coefficients of the powers of ϵ are collected, and all but the coefficients of ϵ^k , $k = 1, 2, 3, 4$, are set to zero. Then, ϵ is set equal to 1. This results in the fourth-order, nonlinear PDE for $h(x, t)$:

$$\begin{aligned} h_t = & BM(0)(15\epsilon_\gamma - 1 + (1 - G - 15\epsilon_\gamma)e^{-h})h_{xxxx} \\ & + (AM'(0) - BM(0)(1 - G + \epsilon_\gamma)e^{-h})h_{xx} \\ & - Ah_{xx}(M(0)h_x + \frac{3}{2}h_x^2M'(0)) + Be^{-h}F, \end{aligned} \quad (7)$$

where

$$\begin{aligned} F = & M'(0)h_x^3(1 - G + \epsilon_\gamma) - 2M'(0)h_xh_{xx}(1 - G + \epsilon_\gamma) - M(0)h_x^4(1 - G - 7\epsilon_\gamma) \\ & + M(0)h_x^2(1 - G + \epsilon_\gamma) + 5M(0)h_x^2h_{xx}(1 - G - \frac{5}{5}\epsilon_\gamma) \\ & - 3M(0)h_xh_{xxx}(1 - G - 15\epsilon_\gamma) - 2M(0)h_{xx}^2(1 - G - 15\epsilon_\gamma). \end{aligned} \quad (8)$$

The first and second lines of (7) are composed of the linear contributions, while all terms in the third line are nonlinear (i.e., they are proportional to the products of the spatial derivatives of h). The terms in the first line emerge due to the natural diffusions of adatoms, mediated by a surface/substrate-interaction force, on a heated crystal surface with anisotropic surface energy. In the second line, the linear term that is proportional to B is also due to the natural diffusion mediated by the wetting effect, while another linear term there that is proportional to A is due to the electromigration drift of adatoms. In the third line, the two terms that are proportional to A also are due to the electromigration. Finally, the last contribution in the third line, $Be^{-h}F$, is the nonlinearity produced by the substrate wetting effect. This contribution, as well as the linear terms that are proportional to e^{-h} in the first and second lines of (7), drop out in the limit of a thick film, $h \rightarrow \infty$, where the film surface/substrate-interaction force vanishes. When $\epsilon_\gamma = 0$, equations (7) and (8) are reduced to [Khenner 2013, (15)]. In the following, it is important that the coefficients of the linear terms are negative, due to negativity of $M'(0)$ and weak anisotropy, $0 < \epsilon_\gamma < \frac{1}{15}$.

2.1. Example: analysis of a linear second-order PDE. Equation (7) is a well-posed, fourth-order, nonlinear parabolic PDE. The prototype *linear* fourth-order parabolic PDE is

$$h_t = \alpha_1 h_{xxxx} + \alpha_2 h_{xx}, \quad \alpha_1, \alpha_2 < 0. \quad (9)$$

This equation has the trivial solution $h(x, t) = h_0 = \text{const}$. In the physical context, this solution corresponds to a constant-height film for all values of x and t , that is, a film with a planar stationary surface. We call such a solution an equilibrium surface. The key issue is whether the equilibrium is stable or unstable with respect to small perturbations $\xi(x, t)$. This can be settled by substituting $h = h_0 + \xi(x, t)$ and then assuming $\xi(x, t)$ is a single Fourier mode: $\xi(x, t) = \xi_0 e^{\omega t} e^{ikx}$, where ξ_0 is the amplitude, $\omega(k)$ is the growth rate, and k is the wavenumber. (The wavelength, or

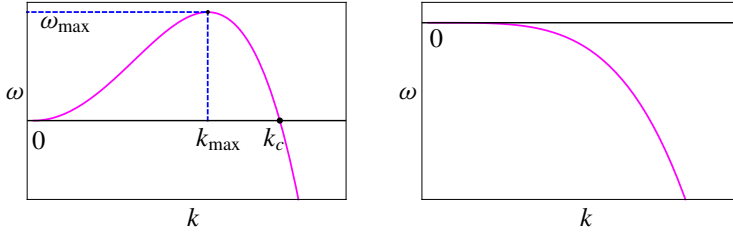


Figure 2. Two cases of the typical growth rate $\omega(k)$. Left: long-wave instability. Right: stability, $\omega(k) < 0$ for all k .

the spatial period, is $\lambda = 2\pi/k$.) Then one obtains the expression for the perturbation growth rate as a function of the wavenumber, the so-called dispersion relation

$$\omega(k) = \alpha_1 k^4 - \alpha_2 k^2. \tag{10}$$

For small k , the second term is dominant in this expression. For large k , it is the first term. Since $\alpha_2 < 0$, perturbations with small wavenumbers (large wavelengths) grow ($\omega(k) > 0$); because $\alpha_1 < 0$, perturbations with large wavenumbers (small wavelengths) decay ($\omega(k) < 0$). This is reflected in the shape of the curve $\omega(k)$ (see Figure 2 (left)), and correspondingly the instability is termed the *long-wavelength instability*. All perturbations with wavenumbers in the interval $0 < k < k_c$ grow, and all perturbations with wavenumbers greater than k_c decay; k_c is termed the *instability cut-off wavenumber*. The surface is unstable with respect to long-wavelength perturbations, and it is stable with respect to small-wavelength perturbations. In practice, the perturbation (induced, for instance, by a thermal noise) is not a single Fourier mode. However, most perturbations can be represented by a superposition of Fourier modes. Thus some modes grow and some decay. Among the unstable modes, there is a mode with the largest growth rate, ω_{\max} . This *most dangerous* mode will dominate over other modes shortly after the surface is destabilized, resulting in a surface deformation of the form $h(x, t) = h_0 + \xi_0 e^{\omega_{\max} t} \cos k_{\max} x$. Here, k_{\max} is the wavenumber for which $\omega = \omega_{\max}$, i.e., the maximum of $\omega(k)$ on the interval $0 \leq k \leq k_c$. In other words, k_{\max} is the positive solution of $d\omega/dk = 0$.

It is easy to show that for (10), we have $k_{\max} = k_c/\sqrt{2}$. First, we set the right-hand side of (10) to zero and solve for k :

$$\omega(k) = -\alpha_2 k^2 + \alpha_1 k^4 = 0 \implies k^2(-\alpha_2 + \alpha_1 k^2) = 0 \implies k = 0 \text{ or } k = \pm\sqrt{\alpha_2/\alpha_1}.$$

Since we need a positive solution, $k_c = \sqrt{\alpha_2/\alpha_1}$. To determine k_{\max} , we solve $d\omega/dk = 0$ for k ; that is,

$$-2\alpha_2 k + 4\alpha_1 k^3 = 0 \implies 2k(-\alpha_2 + 2\alpha_1 k^2) = 0 \implies k = 0 \text{ or } k = \pm\sqrt{\alpha_2/2\alpha_1}.$$

Again we take the positive solution. Thus, $k_{\max} = \sqrt{\alpha_2/2\alpha_1} = k_c/\sqrt{2}$.

Notice that the parameter α_1 in (9) cannot be positive. Otherwise, the short-wavelength perturbations will grow, which is not physically permissible, since in this case the surface is always unstable — such perturbations would be always present in the spectrum. However, an instability is not universal, and most material surfaces remain planar. Mathematically, (9) in the case of $\alpha_1 > 0$ is ill-posed; despite its higher order, it is similar to the (ill-posed) backward heat equation $h_t = -h_{xx}$. However, the parameter α_2 may be positive for some physical parameters' values. Then $\omega(k)$ is negative for all k (Figure 2 (right)), meaning that all perturbations decay and the surface restores its initial planar shape.

Equations such as (7) are nonlinear; thus the exponential growth of the most dangerous mode will not continue forever. Nonlinear terms in the equation will dampen growth, which usually results in a stationary, nontrivial solution which has the spatial form resembling the large-amplitude cosine curve. Determination of the stability of (7) and the form of the stationary solution will be discussed next.

3. Linear stability analysis

The dynamics of the film surface are governed by the nonlinear PDE (7). Toward our goal of determining stability of the surface with respect to small perturbations, we notice that (7) has the equilibrium solution $h = h_0 = \text{const.}$, and we linearize about this solution along the lines described above for (9). First, using the general small perturbation $\xi(x, t)$, we substitute $h = h_0 + \xi(x, t)$ in (7) and retain only the linear terms in ξ . Then, we substitute $\xi = \xi_0 e^{\omega t} e^{ikx}$, calculate the partial derivatives and divide out the factor $\xi_0 e^{\omega t}$. This results in the dispersion relation

$$\omega(k) = -BM(0)((G - 1 + 15\epsilon_\gamma)e^{-h_0} + 1 - 15\epsilon_\gamma)k^4 - (BM(0)(G - 1 - \epsilon_\gamma)e^{-h_0} + AM'(0))k^2. \quad (11)$$

3.1. Analysis of the dispersion relation (11). In this section we determine how the physical parameters of the problem affect the surface instability.

As we explained in Section 2, if $\omega(k) < 0$ for all k , then the surface is stable with respect to the perturbations of any wavenumber (Figure 2 (right)). When this condition does not hold, the surface is long-wave unstable (Figure 2 (left)). The degree of the instability is measured by the width of the domain under the dispersion curve $\omega(k)$. That is, the larger the cut-off wavenumber k_c is, the stronger the instability.

We notice that the dispersion relation (11) has the form of (10) and thus we identify

$$\begin{aligned} \alpha_1 &= -BM(0)((G - 1 + 15\epsilon_\gamma)e^{-h_0} + 1 - 15\epsilon_\gamma), \\ \alpha_2 &= BM(0)(G - 1 - \epsilon_\gamma)e^{-h_0} + AM'(0). \end{aligned}$$

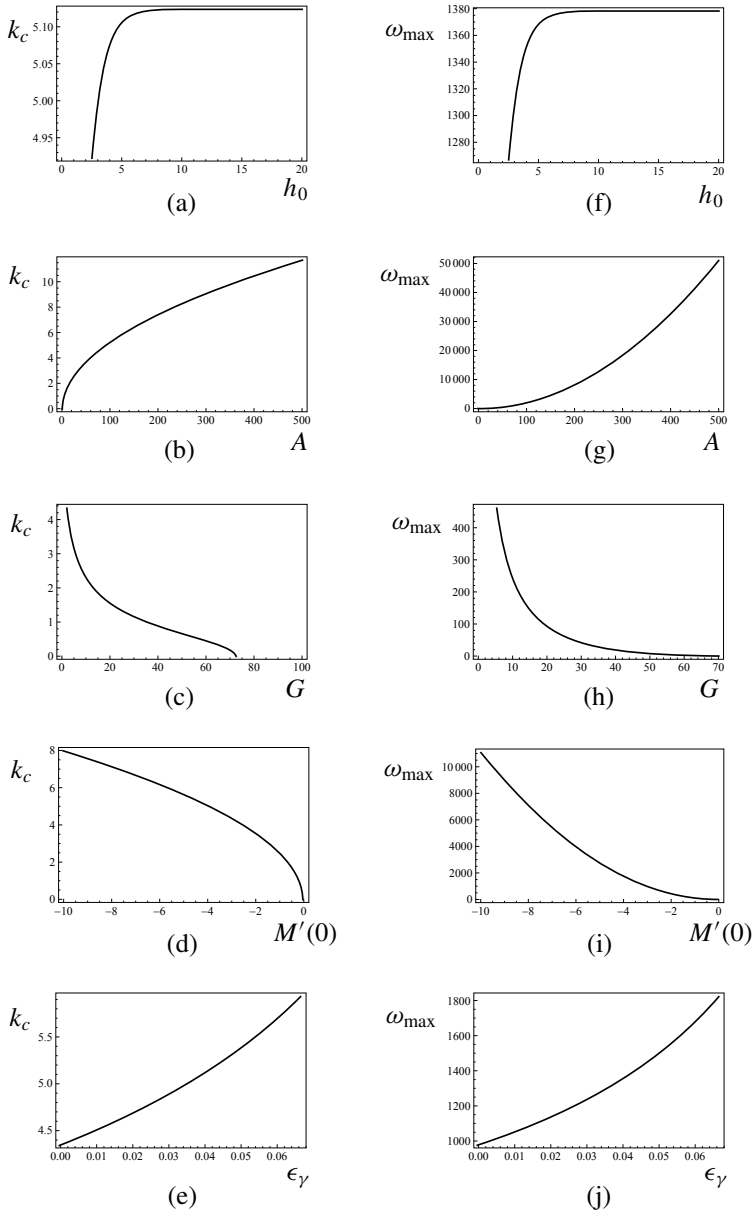


Figure 3. Characterization of the film linear stability. (a) k_c vs. h_0 ; (b) k_c vs. A ; (c) k_c vs. G ; (d) k_c vs. $M'(0)$; (e) k_c vs. ϵ_γ . In (f)–(j), ω_{\max} is plotted vs. the same variables. In each panel, all parameters except the single one that is varied are fixed to the typical values from the second column of Table 1. In (a)–(j), ϵ_γ is chosen equal to zero (isotropic evolution). The same strategy with regard to parameters is followed in Figures 4 and 5.

Then the expressions for k_c , k_{\max} and ω_{\max} are

$$k_c = \sqrt{\frac{Ae^{h_0}M'(0) + BM(0)(G - 1 - \epsilon_\gamma)}{BM(0)(1 - G - 15\epsilon_\gamma + (15\epsilon_\gamma - 1)e^{h_0})}}, \quad k_{\max} = \frac{k_c}{\sqrt{2}}, \quad (12)$$

$$\omega_{\max} = \frac{1}{4} \frac{(Ae^{h_0}M'(0) + BM(0)(G - 1) - BM(0)\epsilon_\gamma)^2}{BM(0)e^{h_0}(G - 1 + 15\epsilon_\gamma + (1 - 15\epsilon_\gamma)e^{h_0})}.$$

The wavelength of the most dangerous perturbation is $\lambda_{\max} = 2\pi/k_{\max}$.

The expressions for k_c , k_{\max} and ω_{\max} include new contributions due to the surface energy anisotropy (the terms proportional to ϵ_γ).

The film stability *decreases* with increasing h_0 , and this trend saturates around $h_0 = 5.12$ nm (Figure 3(a)). This is because the film wets the substrate and thus the attractive, cohesive force between the adatoms and the substrate atoms is stronger for thinner films (smaller h_0). Increasing the electric field strength A also makes the film less stable, but increasing G makes it more stable, since the substrate energy provides a stabilizing effect (Figures 3(b)–(c)). The stability of the film *decreases* with increasing $|M'(0)|$ and ϵ_γ (Figures 3(d)–(e)). The results in the panels (a)–(d) and (f)–(i) were obtained also in [Khenner 2013]; here these results are recomputed from (7). The results in the panels (e) and (j) are new; they stem from the new feature of the extended model: the accounting for the mild anisotropy of the film-surface energy.

4. Numerical solution of equation (7)

Using the information from the previous section on how the physical parameters affect the surface stability, in this section we compute the full nonlinear PDE (7) by implementing the method of lines (MOL) [Verwer and Sanz-Serna 1984; Schiesser 1994] in *Mathematica* [Wolfram 2016]. The MOL is a technique for solving partial differential equations by discretizing in all but one dimension, and then integrating the semidiscrete problem as a system of ordinary differential equations (ODEs). A significant advantage of the method is that it allows us to use the sophisticated general-purpose software [Hairer and Wanner 1999; Brown et al. 1989] that has been developed for numerically integrating large systems of ODEs. For the parabolic initial-boundary-value problems, the MOL typically is very efficient and accurate. Sophisticated adaptive MOL methods were also developed for some hyperbolic equations [Saucez et al. 2001].

The initial condition is the perturbation of $h = h_0$, and the boundary conditions are periodic:

$$h(x, 0) = h_0 + \delta \cos(k_{\max}x), \quad h(0, t) = h(\lambda_{\max}, t), \quad h'(0, t) = h'(\lambda_{\max}, t), \quad (13)$$

where δ is a small amplitude (we take $\delta = 0.01$). Periodic boundary conditions are used since the goal is to compute the evolution of a finite section of a periodic,

laterally unbounded surface. Notice that $h(x, 0)$ is the most dangerous (fastest growing) unstable perturbation according to the linear stability analysis in Section 3.

Evolution of the perturbation is computed until the steady-state solution emerges. The steady-state solution is either a stationary or a traveling wave of wavelength λ_{\max} and constant amplitude. The amplitude and wave speed are studied as a function of the parameters A , h_0 , G , $M'(0)$, and ϵ_γ . It is important to emphasize here that the traveling wave is a nonlinear effect (which was overlooked in [Khenner 2013]); indeed, the perturbation growth rate $\omega(k)$ is real-valued (see (11)), indicating the absence of a linear traveling wave. In computations, the profile started to shift laterally only when the amplitude of a cosine-like perturbation became fairly large, indicating that nonlinearities in (7) are responsible. Another important observation is that for thick films, $h \gg 1$, the wave speed is zero; thus the traveling wave solution is caused by the nonlinear effect of substrate wetting, which is described by the term $Be^{-h}F$ in (7). The lateral drift of surface perturbations has been noted previously in surface electromigration problems; for instance, the drift is the hallmark of [Krug and Schimschak 1997], where it is caused by the nonlocality of the electric field.

Two sets of simulations are conducted, at different film heights: $h_0 = 3$ and $h_0 = 10$; when one parameter is varied, other parameters are fixed to their typical values in Table 1. In addition, the height is also varied with all other parameters fixed. The results are displayed in Figures 4 and 5.

Figures 4(a)–(b) show the effect of varying the film height on the amplitude and the wave speed. Both graphs show the sharp decreases and then the amplitude levels off, while the wave speed vanishes at $h_0 \approx 7$. The decrease of the wave amplitude and speed is expected, since the wetting potential and the corresponding driving force decay exponentially as the film thickness increases.

As seen in Figures 4(e) and 5(e), as the electric field parameter A is increased, the amplitude is decreased and then it levels off. As the graph is the same, we conclude that the dependence of the amplitude on A is unaffected (or is affected very weakly) by the height changes and by the traveling surface wave. Changing A affects the wave speed in a more complicated manner. As Figure 5(f) shows, increasing the strength of the field initially dampened the wave speed, but with further increase of the field, the wave speed also increases. The latter behavior is expected, since the strong field implies a fast adatoms drift. We will be looking into the reason for the initial wave speed decrease.

Figures 4(c) and 5(a) show that increasing the anisotropy strength ϵ_γ makes the amplitude smaller. The wave speed, however, increases with the increase of ϵ_γ , as shown in Figure 5(b). The amplitude variation is primarily affected by ϵ_γ and the simultaneous height changes make little difference.

In Figure 5(g), the amplitude increases only very little as the ratio of the energies G increases. (At $h_0 = 10$, the amplitude value stays constant (≈ 0.65) as G is

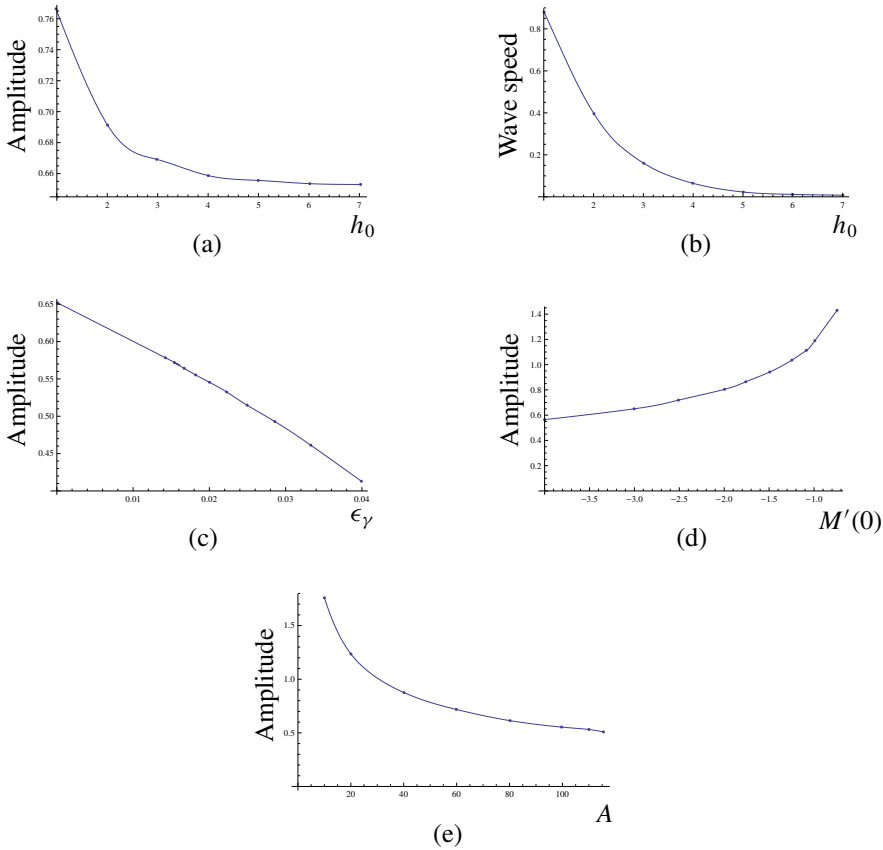


Figure 4. Graphs (a)–(b) show the effects of varying h_0 on the traveling wave amplitude and speed. Graphs (c)–(e) show the effects of varying ϵ_γ , $M'(0)$ and A on the stationary wave amplitude; here $h_0 = 10$, i.e., the film is thick. As is displayed in (b), for thick films the wave speed is zero.

varied; thus this graph is not shown in Figure 4.) In Figure 5(h), the wave speed increases as G increases.

Increasing the absolute value of the diffusional mobility derivative, $|M'(0)|$, results in the decrease of the amplitude and wave speed, as shown in Figures 4(d), 5(c) and 5(d). Once again we notice that the height variation does not seem to affect the trends that $M'(0)$ places on these characteristics.

Notice from the graphs of the amplitude in Figures 4 and 5 that the amplitude never reaches the value of h_0 , that is, 3 or 10. This means that the film’s local height is not zero, and therefore the film does not dewet the substrate. In other words, the film continuously covers the substrate at all times—the substrate is

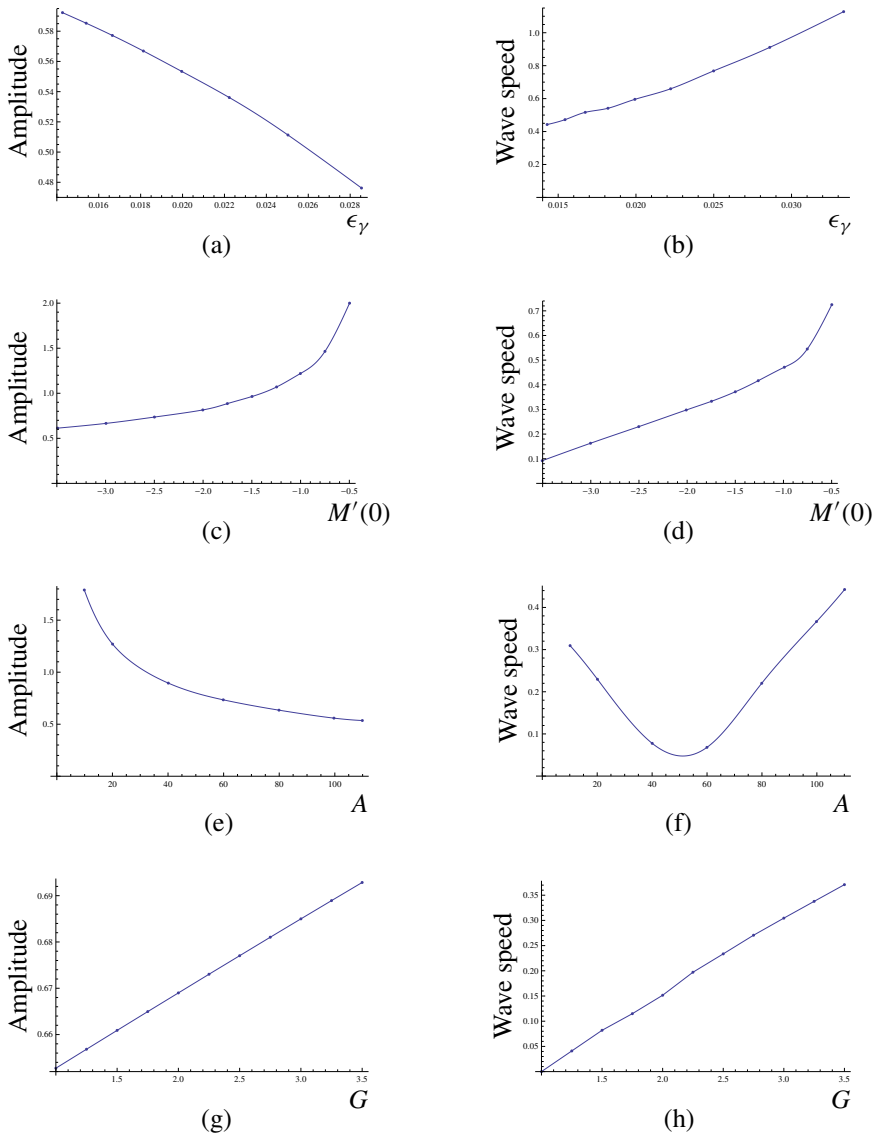


Figure 5. The effects of the parameters’ variation on the traveling wave amplitude and speed (the first and second column, respectively), for the thin film ($h_0 = 3$).

not exposed, despite the application of the electromigration. This can be expected, since the electric field is applied along the substrate, rather than across it. In the latter situation the film is more likely to dewet [Khenner 2013].

These results give insights into the complicated nonlinear dynamics of a film surface. Importantly, even though increasing A , ϵ_γ and $|M'(0)|$ results in the

decrease of the amplitude, the initial state of $\delta = 0.01$ is never reached. Thus at all times $t > 0$ the surface is always more deformed than it is initially.

The amplitude trends shown in Figures 4(a),(d),(e) and Figures 5(c),(e),(g) confirm the results obtained previously in [Khenner 2013]. The results for the amplitude and wave speed in other panels of these figures are new. As we noted above, the traveling wave solution was overlooked in [Khenner 2013] and thus the dependence of the traveling wave speed and amplitude on parameters, including the new parameter, i.e., the strength of the anisotropy ϵ_γ , was not computed there.

5. Conclusions

We performed the analysis of the partial differential equation model of the surface morphological evolution affected by electromigration, assuming a wetting solid film with the mildly anisotropic surface energy.

The linear stability analysis shows that the stability of the base planar state of the surface decreases with the increasing film thickness h_0 , the electric field strength A , the derivative of the diffusional mobility $|M'(0)|$ and the anisotropy strength ϵ_γ . The stability increases with increasing the ratio G of the substrate energy to the film energy, or equivalently, increasing the strength of the intermolecular attractive force between the adatoms and the atoms of the substrate.

We used the method of lines to numerically solve the fully nonlinear PDE. This way we found two outcomes of the surface evolution: the stationary wave relief for thick films, and the traveling surface wave (the surface drift) for thin films. We illustrated how all other physical parameters affect the amplitude of either wave (stationary or traveling), as well as the wave speed of the traveling wave. Our results also hint that there is no combination of the physically admissible parameters' values for which the film dewets the substrate.

Our numerical studies are on the periodic one-wavelength domain $x \in [0, \lambda_{\max}]$, and we used the cosine curve with the small initial amplitude to perturb the (constant) initial height. Future work will be focused on computing the evolution of a small random perturbation on the large periodic domain comprising many wavelengths. In this setup, the coarsening of the initial perturbation can be studied and predictions can be made about the pattern formation on the surface.

Acknowledgments

Aaron Wingo would like to thank his family and friends for all their support, but especially Dr. Khenner for his patience and guidance.

References

[Averbuch et al. 2001] A. Averbuch, E. Glickman, M. Israeli, M. Khenner, and M. Nathan, "Level set modeling of transient electromigration grooving", *Comp. Mater. Sci.* **20** (2001), 235–250.

- [Barakat et al. 2012] F. Barakat, K. Martens, and O. Pierre-Louis, “Nonlinear wavelength selection in surface faceting under electromigration”, *Phys. Rev. Lett.* **109**:5 (2012), Article ID #056101.
- [Barnes et al. 2010] C. H. W. Barnes, A. B. Dominguez, L. L. Felix, S. I. Khondaker, Y. Majima, T. Mitrelias, F. Sfigakis, and L. Valladares, “Controlled electroplating and electromigration in nickel electrodes for nanogap formation”, *Nanotechnology* **21** (2010), Article ID #445304.
- [Block et al. 2006] T. Block, G. Gardinowski, H. Pfnür, J. Schmeidel, and C. Tegenkamp, “Switchable nanometer contacts: ultrathin Ag nanostructures on Si(100)”, *Appl. Phys. Lett.* **89**:6 (2006), Article ID #063120.
- [Bolotin et al. 2007] K. I. Bolotin, F. Kuemmeth, D. C. Ralph, and T. Taychatanapat, “Imaging electromigration during the formation of break junctions”, *Nano Lett.* **7** (2007), 652–656.
- [Brown et al. 1989] P. N. Brown, G. D. Byrne, and A. C. Hindmarsh, “VODE: a variable-coefficient ODE solver”, *SIAM J. Sci. Stat. Comput.* **10**:5 (1989), 1038–1051. MR 1009555 Zbl 0677.65075
- [Cahn and Taylor 1994] J. W. Cahn and J. E. Taylor, “Linking anisotropic sharp and diffuse surface motion laws via gradient flows”, *J. Stat. Phys.* **77**:1–2 (1994), 183–197. MR 1300532 Zbl 0844.35044
- [Cahn et al. 1992] J. W. Cahn, C. A. Handwerker, and J. E. Taylor, “Geometric models of crystal growth”, *Acta Met. Mat.* **40** (1992), 1443–1474.
- [Chang et al. 2006] J. Chang, C. Misbah, and O. Pierre-Louis, “Birth and morphological evolution of step bunches under electromigration”, *Phys. Rev. Lett.* **96**:19 (2006), Article ID #195901.
- [Dai et al. 2014] S. Dai, R. Yu, J. Zhao, and J. Zhu, “Kinetic faceting of the low index W surfaces under electrical current”, *Surf. Sci.* **625** (2014), 10–15.
- [Davis et al. 2004] S. H. Davis, A. A. Golovin, M. S. Levine, and T. V. Savina, “Faceting instability in the presence of wetting interactions: a mechanism for the formation of quantum dots”, *Phys. Rev. B* **70**:23 (2004), Article ID #235342.
- [Debierre et al. 2007] J.-M. Debierre, M. Dufay, and T. Frisch, “Electromigration-induced step meandering on vicinal surfaces: nonlinear evolution equation”, *Phys. Rev. B* **75**:4 (2007), Article ID #045413.
- [Di Carlo et al. 1992] A. Di Carlo, M. E. Gurtin, and P. Podio-Guidugli, “A regularized equation for anisotropic motion-by-curvature”, *SIAM J. Appl. Math.* **52**:4 (1992), 1111–1119. MR 1174049 Zbl 0800.73021
- [Dobbs and Krug 1994] H. T. Dobbs and J. Krug, “Current-induced faceting of crystal surfaces”, *Phys. Rev. Lett.* **73**:14 (1994), 1947–1950.
- [Gill and Wang 2008] S. P. A. Gill and T. Wang, “On the existence of a critical perturbation amplitude for the Stranski–Krastanov transition”, *Surf. Sci.* **602** (2008), 3560–3568.
- [Hairer and Wanner 1999] E. Hairer and G. Wanner, “Stiff differential equations solved by Radau methods”, *J. Comput. Appl. Math.* **111**:1-2 (1999), 93–111. MR 1730588 Zbl 0945.65080
- [Khenner 2008a] M. Khenner, “Comparative study of a solid film dewetting in an attractive substrate potentials with the exponential and the algebraic decay”, *Math. Model. Nat. Phenom.* **3**:5 (2008), 16–29. MR 2477312 Zbl 06544732
- [Khenner 2008b] M. Khenner, “Morphologies and kinetics of a dewetting ultrathin solid film”, *Phys. Rev. B* **77**:24 (2008), Article ID #245445.
- [Khenner 2013] M. Khenner, “Analysis of a combined influence of substrate wetting and surface electromigration on a thin film stability and dynamical morphologies”, *C. R. Physique* **14** (2013), 607–618.
- [Khenner et al. 2011] M. Khenner, M. Levine, and W. T. Tekalign, “Stability of a strongly anisotropic thin epitaxial film in a wetting interaction with elastic substrate”, *Eur. Phys. Lett.* **93**:2 (2011), Article ID #26001.

- [Krug and Schimschak 1997] J. Krug and M. Schimschak, “Surface electromigration as a moving boundary value problem”, *Phys. Rev. Lett.* **78** (1997), 278–281.
- [Liu and Metiu 1993] F. Liu and H. Metiu, “Dynamics of phase separation of crystal surfaces”, *Phys. Rev. B* **48**:9 (1993), Article ID #5808.
- [Maroudas 1995] D. Maroudas, “Dynamics of transgranular voids in metallic thin films under electromigration conditions”, *Appl. Phys. Lett.* **67** (1995), 798–800.
- [Mullins 1963] W. W. Mullins, “Solid surface morphologies governed by capillarity”, pp. 17 in *Metal surfaces: structure, energetics and kinetics*, American Society for Metals, Cleveland, OH, 1963.
- [Saucez et al. 2001] P. Saucez, W. E. Schiesser, and A. Vande Wouwer (editors), *Adaptive method of lines*, Chapman and Hall, Boca Raton, FL, 2001. MR 1851429 Zbl 0986.65083
- [Schiesser 1994] W. E. Schiesser, *Computational mathematics in engineering and applied science: ODEs, DAEs, and PDEs*, CRC, Boca Raton, FL, 1994. MR 1272015 Zbl 0857.65083
- [Stoyanov 1997] S. Stoyanov, “Current-induced step bunching at vicinal surfaces during crystal sublimation”, *Surf. Sci.* **370** (1997), 345–354.
- [Verwer and Sanz-Serna 1984] J. G. Verwer and J. M. Sanz-Serna, “Convergence of method of lines approximations to partial differential equations”, *Computing* **33**:3-4 (1984), 297–313. MR 773930 Zbl 0546.65064
- [Wolfram 2016] Wolfram, “Mathematica”, 2016, <http://www.wolfram.com/mathematica>.

Received: 2015-01-28 Revised: 2015-07-08 Accepted: 2015-07-31

aaron_wingo@mymail.eku.edu *Department of Mathematics and Statistics,
Eastern Kentucky University, 521 Lancaster Avenue,
Richmond, KY 40475, United States*

scinar@math.uh.edu *Department of Mathematics, University of Houston,
4800 Calhoun Road, Houston, TX 77004, United States*

kurt.woods774@topper.wku.edu *General Motors Corporation, Bowling Green, KY 42101,
United States*

mikhail.khenner@wku.edu *Department of Mathematics, Western Kentucky University,
1906 College Heights Boulevard, Bowling Green, KY 42101,
United States*

involve

msp.org/involve

INVOLVE YOUR STUDENTS IN RESEARCH

Involve showcases and encourages high-quality mathematical research involving students from all academic levels. The editorial board consists of mathematical scientists committed to nurturing student participation in research. Bridging the gap between the extremes of purely undergraduate research journals and mainstream research journals, *Involve* provides a venue to mathematicians wishing to encourage the creative involvement of students.

MANAGING EDITOR

Kenneth S. Berenhaut Wake Forest University, USA

BOARD OF EDITORS

Colin Adams	Williams College, USA	Suzanne Lenhart	University of Tennessee, USA
John V. Baxley	Wake Forest University, NC, USA	Chi-Kwong Li	College of William and Mary, USA
Arthur T. Benjamin	Harvey Mudd College, USA	Robert B. Lund	Clemson University, USA
Martin Bohner	Missouri U of Science and Technology, USA	Gaven J. Martin	Massey University, New Zealand
Nigel Boston	University of Wisconsin, USA	Mary Meyer	Colorado State University, USA
Amarjit S. Budhiraja	U of North Carolina, Chapel Hill, USA	Emil Minchev	Ruse, Bulgaria
Pietro Cerone	La Trobe University, Australia	Frank Morgan	Williams College, USA
Scott Chapman	Sam Houston State University, USA	Mohammad Sal Moslehian	Ferdowsi University of Mashhad, Iran
Joshua N. Cooper	University of South Carolina, USA	Zuhair Nashed	University of Central Florida, USA
Jem N. Corcoran	University of Colorado, USA	Ken Ono	Emory University, USA
Toka Diagana	Howard University, USA	Timothy E. O'Brien	Loyola University Chicago, USA
Michael Dorff	Brigham Young University, USA	Joseph O'Rourke	Smith College, USA
Sever S. Dragomir	Victoria University, Australia	Yuval Peres	Microsoft Research, USA
Behrouz Emamizadeh	The Petroleum Institute, UAE	Y.-F. S. Pétermann	Université de Genève, Switzerland
Joel Foisy	SUNY Potsdam, USA	Robert J. Plemmons	Wake Forest University, USA
Errin W. Fulp	Wake Forest University, USA	Carl B. Pomerance	Dartmouth College, USA
Joseph Gallian	University of Minnesota Duluth, USA	Vadim Ponomarenko	San Diego State University, USA
Stephan R. Garcia	Pomona College, USA	Bjorn Poonen	UC Berkeley, USA
Anant Godbole	East Tennessee State University, USA	James Propp	U Mass Lowell, USA
Ron Gould	Emory University, USA	József H. Przytycki	George Washington University, USA
Andrew Granville	Université Montréal, Canada	Richard Rebarber	University of Nebraska, USA
Jerold Griggs	University of South Carolina, USA	Robert W. Robinson	University of Georgia, USA
Sat Gupta	U of North Carolina, Greensboro, USA	Filip Saidak	U of North Carolina, Greensboro, USA
Jim Haglund	University of Pennsylvania, USA	James A. Sellers	Penn State University, USA
Johnny Henderson	Baylor University, USA	Andrew J. Sterge	Honorary Editor
Jim Hoste	Pitzer College, USA	Ann Trenk	Wellesley College, USA
Natalia Hritonenko	Prairie View A&M University, USA	Ravi Vakil	Stanford University, USA
Glenn H. Hurlbert	Arizona State University, USA	Antonia Vecchio	Consiglio Nazionale delle Ricerche, Italy
Charles R. Johnson	College of William and Mary, USA	Ram U. Verma	University of Toledo, USA
K. B. Kulasekera	Clemson University, USA	John C. Wierman	Johns Hopkins University, USA
Gerry Ladas	University of Rhode Island, USA	Michael E. Zieve	University of Michigan, USA

PRODUCTION

Silvio Levy, Scientific Editor

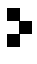
Cover: Alex Scorpan

See inside back cover or msp.org/involve for submission instructions. The subscription price for 2016 is US \$160/year for the electronic version, and \$215/year (+\$35, if shipping outside the US) for print and electronic. Subscriptions, requests for back issues from the last three years and changes of subscribers address should be sent to MSP.

Involve (ISSN 1944-4184 electronic, 1944-4176 printed) at Mathematical Sciences Publishers, 798 Evans Hall #3840, c/o University of California, Berkeley, CA 94720-3840, is published continuously online. Periodical rate postage paid at Berkeley, CA 94704, and additional mailing offices.

Involve peer review and production are managed by EditFLOW® from Mathematical Sciences Publishers.

PUBLISHED BY

 **mathematical sciences publishers**
nonprofit scientific publishing

<http://msp.org/>

© 2016 Mathematical Sciences Publishers

involve

2016

vol. 9

no. 4

Affine hyperbolic toral automorphisms COLIN THOMSON AND DONNA K. MOLINEK	541
Rings of invariants for the three-dimensional modular representations of elementary abelian p -groups of rank four THÉO PIERRON AND R. JAMES SHANK	551
Bootstrap techniques for measures of center for three-dimensional rotation data L. KATIE WILL AND MELISSA A. BINGHAM	583
Graphs on 21 edges that are not 2-apex JAMISON BARSOTTI AND THOMAS W. MATTMAN	591
Mathematical modeling of a surface morphological instability of a thin monocrystal film in a strong electric field AARON WINGO, SELAHITTIN CINAR, KURT WOODS AND MIKHAIL KHENNER	623
Jacobian varieties of Hurwitz curves with automorphism group $\mathrm{PSL}(2, q)$ ALLISON FISCHER, MOUCHEN LIU AND JENNIFER PAULHUS	639
Avoiding approximate repetitions with respect to the longest common subsequence distance SERINA CAMUNGOL AND NARAD RAMPERSAD	657
Prime vertex labelings of several families of graphs NATHAN DIEFENDERFER, DANA C. ERNST, MICHAEL G. HASTINGS, LEVI N. HEATH, HANNAH PRAWZINSKY, BRIAHNA PRESTON, JEFF RUSHALL, EMILY WHITE AND ALYSSA WHITTEMORE	667
Presentations of Roger and Yang's Kauffman bracket arc algebra MARTIN BOBB, DYLAN PEIFER, STEPHEN KENNEDY AND HELEN WONG	689
Arranging kings k -dependently on hexagonal chessboards ROBERT DOUGHTY, JESSICA GONDA, ADRIANA MORALES, BERKELEY REISWIG, JOSIAH REISWIG, KATHERINE SLYMAN AND DANIEL PRITIKIN	699
Gonality of random graphs ANDREW DEVEAU, DAVID JENSEN, JENNA KAINIC AND DAN MITROPOLSKY	715



1944-4176(2016)9:4;1-1